Sciencexpress Reports

Influence of Threonine Metabolism on *S*-Adenosylmethionine and Histone Methylation

Ng Shyh-Chang,[1,2,3,4,5,6] Jason W. Locasale,[5,6]* Costas A. Lyssiotis,[5,6] Yuxiang Zheng,[5,6] Ren Yi Teo,[1] Sutheera Ratanasirintrawoot,[1,2,3] Jin Zhang,[1,2,3] Tamer Onder,[1,2,3] Juli J. Unternaehrer,[1,2,3] Hao Zhu,[1,2,3] John M. Asara,[5] George Q. Daley,[1,2,3,4]† Lewis C. Cantley[5,6]†

[1]Stem Cell Transplantation Program, Division of Pediatric Hematology and Oncology, Manton Center for Orphan Disease Research, Boston Children's Hospital and Dana Farber Cancer Institute, Boston, MA 02115, USA. [2]Department of Biological Chemistry and Molecular Pharmacology, Harvard Medical School, Boston, MA 02115, USA. [3]Harvard Stem Cell Institute, Cambridge, MA 02138, USA. [4]Howard Hughes Medical Institute, Harvard Medical School, Boston, MA 02115, USA. [5]Department of Medicine, Division of Signal Transduction, Beth Israel Deaconess Medical Center, Boston, MA 02215, USA. [6]Department of Systems Biology, Harvard Medical School, Boston, MA 02115, USA.

*Present address: Division of Nutritional Sciences, Cornell University, Ithaca, NY 14850, USA.

†To whom correspondence should be addressed. E-mail: george.daley@childrens.harvard.edu (G.Q.D.); lewis_cantley@hms.harvard.edu (L.C.C.)

Threonine is the only amino acid critically required for the pluripotency of mouse embryonic stem cells (mESCs) but by an unknown mechanism. We demonstrate that threonine (Thr) and *S*-adenosylmethionine (SAM) metabolism are coupled in pluripotent stem cells, resulting in regulation of histone methylation. Isotope labeling of mESCs revealed that Thr provides a significant fraction of both the cellular glycine (Gly) and the acetyl-CoA needed for SAM synthesis. Depletion of Thr from the culture medium or threonine dehydrogenase (Tdh) from mESCs decreased accumulation of SAM and decreased tri-methylation of histone H3 lysine-4 (H3K4me3), leading to slowed growth, and increased differentiation. Thus abundance of SAM appears to influence H3K4me3, providing a possible mechanism by which modulation of a metabolic pathway might influence stem cell fate.

Connections between pluripotency and the metabolic state of mouse embryonic stem cells (mESCs) are only beginning to be described (*1*). Metabolically, mESCs are characterized by a distinct mode of amino acid catabolism driven by the enzyme that catalyzes Thr oxidation, threonine dehydrogenase (Tdh) (*1*). Tdh is over 200 times higher in mESCs than mouse embryonic fibroblasts (MEFs), and Thr restriction or Tdh inhibition abolishes mESC growth (*1*–*3*). Thus Thr oxidation appears to be critical for mESCs, but the relationship between downstream metabolites and the pluripotent state remains unclear.

To investigate how metabolism is altered upon reprogramming to the pluripotent state, we used liquid chromatography-based tandem mass spectrometry (LC-MS/MS) (*4*) to profile metabolomic changes during reprogramming into induced pluripotent stem cells (iPSCs). We used MEFs transfected with doxycycline-activated transgenes encoding Oct4, Sox2, Klf4, and Myc (OSKM) (*2*, *5*) and profiled metabolism during reprogramming. Hierarchical clustering based on the abundance of each metabolite revealed that iPSCs were similar to mESCs, and distinct from MEFs (Fig. 1, A and B). Inspection of the top metabolites regulated by OSKM-induced reprogramming revealed a large number of glycolytic intermediates (fig. S1A and table S1), many of which were significantly more abundant within just 4 days of reprogramming (Fig. 1C), when proliferation was accelerated but the cells were not yet pluripotent (*2*). Thus increases in glycolytic intermediates occurred before acquisition of pluripotency (Fig. 1C). The other top metabolites regulated during reprogramming are involved in threonine (Thr) and *S*-adenosylmethionine (SAM) metabolism. In contrast to glycolytic intermediates, Thr- and SAM-related metabolites changed late in reprogramming, suggesting that enhanced Thr and SAM metabolism accompanied acquisition of the pluripotent state (Fig. 1D). Upon reprogramming, some of the largest decreases were in Thr, Cys and folate, and the largest increases were in SAM and cystathionine.

Metabolism is also rewired during mESC differentiation. In mESCs, the *let-7* microRNA promotes differentiation by suppressing the pluripotency network, whereas *Lin28a* promotes pluripotency by repressing *let-7* (*6*, *7*). Hence we profiled metabolic changes in mESCs acutely after dox-induced activation of a transgene encoding *let-7* or *Lin28a* (iLet-7 or iLin28a), while the cell-cycle remained unperturbed (fig. S1B). *Lin28a* and *let-7* regulated 38 metabolites in a reciprocal manner (fig. S1C), among which were a large number of Thr and SAM metabolites (Fig. 1E), further supporting the idea that Thr and SAM metabolism are coupled to pluripotency.

We integrated our metabolomics data on mESCs (table S1) with cDNA microarray data on mESCs (*2*) using the KEGG database of metabolic networks. This analysis showed that many of the metabolic enzymes that channel Thr metabolism into SAM metabolism, e.g., Tdh, Gcat, Gldc, Dhfr, Fol1r, Mat2a/b and Ahcy, are much higher in mESCs than MEFs (Fig. 2A). Consistent with the enzyme expression patterns, several Thr-SAM pathway inputs like Thr, Cys, and folate were less abundant in mESCs than in MEFs, whereas downstream outputs like SAM and cystathionine were more abundant in mESCs than MEFs (Fig. 1D). Thus a Thr-SAM pathway appears to be activated in mESCs.

To test this pathway, we traced the metabolic fate of ^{14}C-Thr in mESCs with HPLC. ^{14}C-isotope was incorporated into Gly and Glu, indicating that Thr was used to synthesize these amino acids (Fig. 2B). In contrast, MEFs incubated with ^{14}C-Thr did not exhibit Thr catabolism (fig. S2A). We also traced the fate of ^{13}C-Thr in mESCs with LC-MS/MS metabolomics (fig. S2, B to F, and table S1). mESCs used Thr to synthesize acetyl-CoA-derived TCA cycle intermediates (Fig. 2, C and D). At steady-state, ^{13}C-Thr contributed ~20% of the citrate via acetyl-CoA, whereas ^{13}C-glucose contributed ~35% via acetyl-CoA (+2 isotopomer). Thus Thr contributes significantly to the acetyl-CoA pool in mESCs (Fig. 2D). Extracellular ^{13}C-Thr-derived ^{13}C-Gly also donated its ^{13}C-methyl group to ultimately generate 5-methyl-tetrahydrofolate (5mTHF) and SAM (+1 isotopomer), whereas extracellular ^{13}C-Ser-derived ^{13}C-Gly contributed little to the synthesis of these metabolites (Fig. 2, C and D). Although only ~25% of intracellular Gly and 5mTHF, and ~10% of SAM were labeled by ^{13}C-Thr at steady state, these numbers underestimate the contribution of Thr to the synthesis of these intermediates due to rapid 1-for-1 antiport of intracellular ^{13}C-Gly and ^{13}C-Met for extracellular ^{12}C-Gly and ^{12}C-Met. Evidence for rapid antiport-mediated ^{13}C-isotope dilution was provided by the appearance of large quantities of ^{13}C-Gly and ^{13}C-Met in the media - 6% of extracellular Gly

and 13% of extracellular Met was ^{13}C-labeled within 1 hour of ^{13}C-Thr addition to the media - with no significant consumption of Gly or Met from the media. (fig. S2I). These data suggest that the rapid conversion of Thr to Gly by Tdh provides a major fraction of 5mTHF needed for recycling SAH to SAM.

To test whether Thr was indeed a major fuel source for Gly and SAM metabolism, we profiled metabolic changes upon Thr restriction in mESCs; all the Thr in DMEM medium was removed, but there remained enough Thr in the serum for cellular protein synthesis (*1*, *8*). In fact, Thr restriction affected mESC viability additively with, and thus independently of protein synthesis (fig. S2, G and H). The 80% drop in intracellular Thr caused intracellular Gly and the SAM/SAH ratio to decrease steadily, suggesting an imbalance in Gly synthesis and consumption (Fig. 2, E and F, and table S1). In contrast, glucose-6-phosphate, fructose-6-phosphate, lactate, and the ATP/AMP ratio increased (Fig. 2, E and F), consistent with a compensatory increase in glycolysis. However, some of the TCA cycle intermediates still decreased (fig. S2J). The drop in NADH might indicate a drop in Thr-derived acetyl-CoA, which fuels the TCA cycle's production of reducing equivalents (Fig. 2F and fig. S2, K and L). Thus, our results support the idea that Thr is critically required in mESCs because of its contribution to Gly for 5mTHF and SAM synthesis, and because acetyl-CoA produced from Thr could contribute to this anabolic process (Fig. 2A).

As another test of this model, we attempted to suppress the effects of Thr restriction on mESCs by supplementing the culture medium with downstream metabolites in the Thr-SAM pathway. Addition of Gly and pyruvate (a source of acetyl-CoA), but neither alone, prevented mESC death after Thr restriction (Fig. 2G). Glucose, acetate, Ser, Cys, Glu, Gln, N-acetyl-cysteine, ascorbate or combinations with pyruvate, all failed to prevent mESC death after Thr restriction. However a combination of pyruvate with the methyl donors dimethylglycine or betaine prevented death from Thr restriction (Fig. 2G), suggesting that Thr-derived 5mTHF and its main product SAM (Fig. 2, C and D) are essential for mESCs. SAM could not be used because it cannot cross mammalian plasma membranes (*9*). In contrast 3-deaza-adenosine (DZA) (*10*), which decreases the SAM/SAH ratio by inhibiting SAH hydrolase, did enter mESCs and inhibited mESC viability (fig. S2M). Hypoxanthine and thymidine also failed to prevent mESC death after Thr restriction although they could enter mESCs (*11*), suggesting that nucleosides are not important downstream products of Thr-derived Gly. A downstream product of SAM catabolism, the polyamine spermidine (*12*), was also ineffective. Thus Thr appears to be necessary to generate the optimal balance of Gly and acetyl-CoA required to synthesize 5mTHF, for maintaining the SAM/SAH ratio in mESCs.

SAM is the universal substrate for all protein methylation reactions in the cell, and the SAM/SAH ratio is important for regulating protein methylation because methyltransferases are product-inhibited by SAH (Fig. 3A) (*13*). To test whether Thr restriction affects protein methylation, we used a pan-methyl-lysine antibody to detect differential lysine methylation of proteins after restriction of Thr, Gly, and Ser. Amongst the most abundant methylated proteins (*14*), histone H3 showed a drop in methylation upon Thr restriction, whereas heat shock protein 8, elongation factor-1a and actin showed only subtle changes (Fig. 3B). Because euchromatin is crucial for epigenetic plasticity in mESCs, and because histone H3 lysine-4 tri-methylation (H3K4me3) and H3 acetylation (H3ac) are important for maintaining euchromatin (*15–18*), we tested whether Thr catabolism regulates H3K4me3 and H3ac in mESCs. Under milder conditions of Thr restriction (0.3X) that did not inhibit mESC growth (fig. S3A), H3K4me3 dropped by 48 hours, whereas H3ac remained unchanged (Fig. 3C). In comparison, MEFs showed no changes in H3K4me3 nor H3ac upon 0.3X Thr restriction (Fig. 3C), consistent with our observations that Thr-SAM metabolism is activated only in the pluripotent state.

To test the sensitivity and reversibility of H3K4me3, we supplemented Thr-restricted mESCs with various doses of Thr. Although mESCs lost most of their H3K4me3 after just 6 hours of Thr restriction, re-feeding with various concentrations of Thr for 6 hours reversed the drop in H3K4me3 (fig. S3B). H3K4me3 could also be restored by adding pyruvate and Gly to the medium (Fig. 3D). Both pyruvate and Gly were necessary to restore the SAM/SAH ratio to a normal state, consistent with the idea that Thr-derived acetyl-CoA and Gly regulate H3K4me3 by modulating the SAM/SAH ratio (Fig. 3E). Conversely DZA, which decreases the SAM/SAH ratio, led to a rapid extinction of H3K4me3 and over-rode the effects of pyruvate and Gly on mESCs (Fig. 3, D and E, and fig. S3C), suggesting that the SAM/SAH ratio lies upstream of H3K4me3 and downstream of acetyl-CoA and Gly. We then tested H3 methylation on lysines 4, 9, 27, 36, and 79 in mESCs after restriction of a variety of individual amino acids. H3K4me3 and H3K4me2 were decreased by Thr restriction. H3K4me1, H3K9me3, H3K27me3, H3K36me3 and H3K79me3 did not change significantly with any amino acid (Fig. 3F). Also, α-ketoglutarate did not change significantly during Thr restriction (fig. S2J), suggesting minimal influence on α-ketoglutarate-dependent histone demethylases. These results suggest that the SAM/SAH ratio maintained by Thr catabolism is not required to regulate all protein lysine methylation, but rather certain specific lysines such as H3K4me2 and H3K4me3 in mESCs (Fig. 3F). Assays of total H3K4 methyltransferase activity from nuclear lysates further indicated that the change in H3K4me3 with Thr concentration was not due to a change in the net amount of methyltransferase activity (fig. S3D), supporting the idea that it is the change in the substrate/product ratio (SAM/SAH) that influenced the amount of H3K4me3.

To test whether the Thr-SAM pathway has functional consequences on the pluripotency and differentiation of mESCs, we partially depleted the Tdh enzyme using RNA interference (Fig. 4A and fig. S4A). In low Thr conditions, partial Tdh depletion led to a decrease in mESC growth and an increase in mESC differentiation (Fig. 4B). Expression profiling by qRT-PCR revealed that Tdh depletion led to a decrease in expression of pluripotency factors, including *Oct4, Sox2, Nanog, Rex1,* and *Blimp1,* and increased expression of the differentiation factors *Foxa2* and *Sox17* (fig. S4B). Embryoid body differentiation of the mESCs for 3 days showed that Tdh depletion led to more rapid extinction of the pluripotency factor *Sox2*, and an aberrant increase in transcription of the differentiation factors *Gata4* and *Sox17* (fig. S4C). Importantly, the differentiation of mESCs after partial Tdh depletion was dependent on the amount of Thr in the culture medium, suggesting that Tdh was required for its metabolic function (Fig. 4B). Indeed, Tdh depletion decreased Thr-SAM flux (Fig. 4C). At steady state, Tdh depletion also decreased Gly, citrate, and the SAM/SAH ratio (Fig. 4D). Tdh depletion also decreased H3K4me3 abundance (Fig. 4A). Thus Thr catabolism by Tdh appears to be required for maintenance of the pluripotent epigenetic state. We also tested whether enzymes downstream of Tdh in the Thr-SAM pathway are also required by mESCs, including glycine decarboxylase (Gldc) which produces methylene-THF from Gly (*19*), and methionine adenosyltransferase (Mat2a) which produces SAM from Met. Depletion of Gldc decreased Thr to SAM flux and the level of H3K4me3, and decreased mESC colony growth (fig. S4, D to H). In contrast, transient overexpression of Gldc prevented mESC death after Thr restriction (fig. S4, I and J), suggesting that the 5mTHF and SAM downstream of Thr and Gly are necessary for mESCs. Depletion of the downstream Mat2a also decreased SAM synthesis and H3K4me3 levels, and decreased mESC colony growth (fig. S4, F to H). Conversely, transient overexpression of the SAH hydrolase (Ahcy) which decreases SAH and thereby increases the SAM/SAH ratio, prevented mESC death after Thr restriction (fig. S4, I and J). Finally components of the H3K4 methyltransferase complexes, like Wdr5, Dpy30, and Setd1a also im-

proved mESC survival after Thr restriction, supporting the idea that Thr-SAM metabolism may affect mESCs in part through effects on H3K4me3.

We have demonstrated the Thr-SAM pathway is activated in mouse pluripotent stem cells. Thr-dependent changes in the SAM/SAH ratio correlated with H3K4me3, thus revealing a possible mechanistic link between cellular metabolism and the epigenetic state. The unique activity of Tdh in converting Thr into both Gly and acetyl-CoA appears to optimize the synthesis of SAM to maintain a high SAM/SAH ratio. H3K4me3 was also more sensitive to changes in Thr metabolism than methylation of other histone H3 lysines, possibly due to the high abundance of this H3 methylation mark in the euchromatin of mESCs and its rapid turnover (*15*–*18*, *20*, *21*). In fact H3K4me3 is critical for self-renewal of pluripotent stem cells (*22*). Since dysregulation of Gly metabolism has been implicated in a variety of human cancers (*4*, *19*, *23*, *24*), and the upstream TDH enzyme has been lost by mutation in humans (*1*), our findings might provide insights into a metabolic pathway that is dysregulated during human tumorigenesis.

References and Notes

1. J. Wang *et al*., Dependence of mouse embryonic stem cells on threonine catabolism. *Science* **325**, 435 (2009). doi:10.1126/science.1173288 Medline
2. T. S. Mikkelsen *et al*., Dissecting direct reprogramming through integrative genomic analysis. *Nature* **454**, 49 (2008). doi:10.1038/nature07056 Medline
3. P. B. Alexander, J. Wang, S. L. McKnight, Targeted killing of a mammalian cell based upon its specialized metabolic state. *Proc. Natl. Acad. Sci. U.S.A.* **108**, 15828 (2011). doi:10.1073/pnas.1111312108 Medline
4. J. W. Locasale *et al*., Phosphoglycerate dehydrogenase diverts glycolytic flux and contributes to oncogenesis. *Nat. Genet.* **43**, 869 (2011). doi:10.1038/ng.890 Medline
5. M. Stadtfeld, N. Maherali, D. T. Breault, K. Hochedlinger, Defining molecular cornerstones during fibroblast to iPS cell reprogramming in mouse. *Cell Stem Cell* **2**, 230 (2008). doi:10.1016/j.stem.2008.02.001 Medline
6. S. R. Viswanathan, G. Q. Daley, R. I. Gregory, Selective blockade of microRNA processing by Lin28. *Science* **320**, 97 (2008). doi:10.1126/science.1154040 Medline
7. C. Melton, R. L. Judson, R. Blelloch, Opposing microRNA families regulate self-renewal in mouse embryonic stem cells. *Nature* **463**, 621 (2010). doi:10.1038/nature08725
8. H. Eagle, K. A. Piez, M. Levy, The intracellular amino acid concentrations required for protein synthesis in cultured human cells. *J. Biol. Chem.* **236**, 2039 (1961). Medline
9. J. M. McMillan, U. K. Walle, T. Walle, S-adenosyl-L-methionine: Transcellular transport and uptake by Caco-2 cells and hepatocytes. *J. Pharm. Pharmacol.* **57**, 599 (2005). doi:10.1211/0022357056082 Medline
10. P. S. Backlund, Jr., D. Carotti, G. L. Cantoni, Effects of the S-adenosylhomocysteine hydrolase inhibitors 3-deazaadenosine and 3-deazaaristeromycin on RNA methylation and synthesis. *Eur. J. Biochem.* **160**, 245 (1986). doi:10.1111/j.1432-1033.1986.tb09963.x Medline
11. V. Valancius, O. Smithies, Testing an "in-out" targeting procedure for making subtle genomic modifications in mouse embryonic stem cells. *Mol. Cell. Biol.* **11**, 1402 (1991). Medline
12. D. Zhang *et al*., AMD1 is essential for ESC self-renewal and is translationally down-regulated on differentiation to neural precursor cells. *Genes Dev.* **26**, 461 (2012). doi:10.1101/gad.182998.111 Medline
13. Z. Luka, S. H. Mudd, C. Wagner, Glycine N-methyltransferase and regulation of S-adenosylmethionine levels. *J. Biol. Chem.* **284**, 22507 (2009). doi:10.1074/jbc.R109.019273 Medline
14. H. Iwabata, M. Yoshida, Y. Komatsu, Proteomic analysis of organ-specific post-translational lysine-acetylation and -methylation in mice by use of anti-acetyllysine and -methyllysine mouse monoclonal antibodies. *Proteomics* **5**, 4653 (2005). doi:10.1002/pmic.200500042 Medline
15. A. Gaspar-Maia, A. Alajem, E. Meshorer, M. Ramalho-Santos, Open chromatin in pluripotency and reprogramming. *Nat. Rev. Mol. Cell Biol.* **12**, 36 (2011). doi:10.1038/nrm3036 Medline
16. V. Azuara *et al*., Chromatin signatures of pluripotent cell lines. *Nat. Cell Biol.* **8**, 532 (2006). doi:10.1038/ncb1403 Medline
17. X. D. Zhao *et al*., Whole-genome mapping of histone H3 Lys4 and 27 trimethylations reveals distinct genomic compartments in human embryonic stem cells. *Cell Stem Cell* **1**, 286 (2007). doi:10.1016/j.stem.2007.08.004 Medline
18. G. Pan *et al*., Whole-genome analysis of histone H3 lysine 4 and lysine 27 methylation in human embryonic stem cells. *Cell Stem Cell* **1**, 299 (2007). doi:10.1016/j.stem.2007.08.003 Medline
19. W. C. Zhang *et al*., Glycine decarboxylase activity drives non-small cell lung cancer tumor-initiating cells and tumorigenesis. *Cell* **148**, 259 (2012). doi:10.1016/j.cell.2011.11.050 Medline
20. R. B. Deal, J. G. Henikoff, S. Henikoff, Genome-wide kinetics of nucleosome turnover determined by metabolic labeling of histones. *Science* **328**, 1161 (2010). doi:10.1126/science.1186777 Medline
21. B. M. Zee *et al*., In vivo residue-specific histone methylation dynamics. *J. Biol. Chem.* **285**, 3341 (2010). doi:10.1074/jbc.M109.063784 Medline
22. Y. S. Ang *et al*., Wdr5 mediates self-renewal and reprogramming via the embryonic stem cell core transcriptional network. *Cell* **145**, 183 (2011). doi:10.1016/j.cell.2011.03.003 Medline
23. R. Possemato *et al*., Functional genomics reveal that the serine synthesis pathway is essential in breast cancer. *Nature* **476**, 346 (2011). doi:10.1038/nature10350 Medline
24. M. Jain *et al*., Metabolite profiling identifies a key role for glycine in rapid cancer cell proliferation. *Science* **336**, 1040 (2012). doi:10.1126/science.1218595 Medline

Acknowledgments: We thank members of the Daley and Cantley labs for helpful discussions. N.S.C. is supported by the NSS Scholarship from the Agency for Science, Technology and Research, Singapore. J.W.L is supported by grants from the NIH (4R00CA168997-02) and the American Cancer Society. C.A.L. is the Amgen fellow of the Damon Runyon Cancer Research Foundation. G.Q.D. is supported by grants from the NIH (RC2HL102815 and U01 HL100001), and is an investigator of the HHMI. L.C.C. is supported by grants from both the NIH and NCI. G.Q.D., as a co-founder and member of the SAB, holds stock options and receives consulting fees from iPierian Inc, a biopharmaceutical company that uses iPS cells in drug discovery against neurologic disease. L.C.C. is the founder and a member of the BOD of Agios Pharmaceuticals, a company that targets metabolic enzymes for cancer treatment.

Supplementary Materials

www.sciencemag.org/cgi/content/full/science.1226603/DC1
Materials and Methods
Figs. S1 to S4

26 June 2012; accepted 22 October 2012

Published online 1 November 2012
10.1126/science.1226603

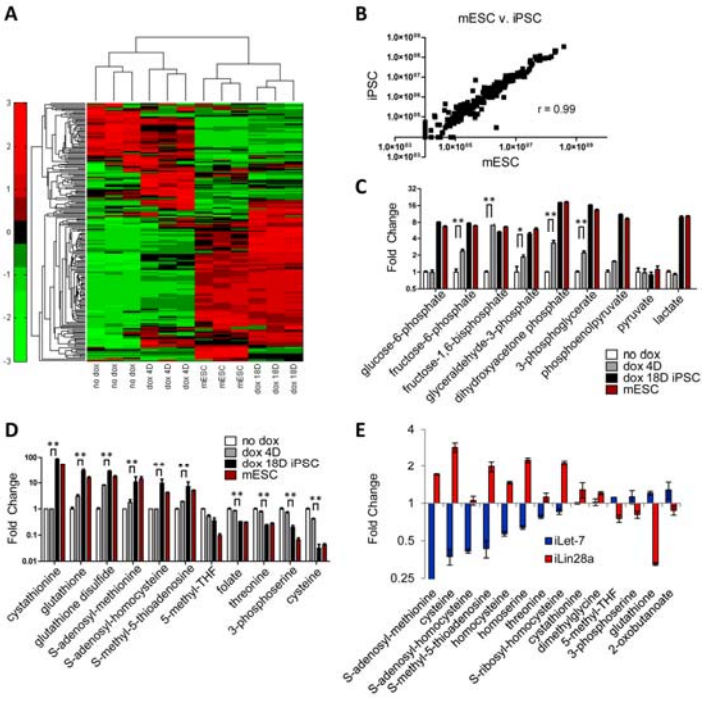

Fig. 1. Thr-SAM pathway is activated by pluripotency factors. (**A**) Heat map showing relative abundance of metabolites in iOSKM-MEFs in the absence of doxycycline treatment (no dox), 4 days after dox (dox 4D), 18 days after dox whereupon iPSC clones are fully reprogrammed (dox 18D), and mESCs, normalized to total biomass (n = 3), and measured using selected reaction monitoring (SRM) and LC-MS/MS. (**B**) Scatter plot of metabolite intensities in mESCs (x-axis) vs. iPSCs (y-axis). Metabolite intensities were obtained from the integrated total ion current from a single SRM transition. (**C**) SRM analysis of abundance in glycolytic intermediates in iOSKM-MEFs during reprogramming (n = 3). ***P*< 0.01, * *P*< 0.05. (**D**) SRM analysis of abundance in Thr-SAM pathway intermediates in iOSKM-MEFs during reprogramming (n = 3). ** *P*< 0.01. (**E**) SRM analysis of abundance in Thr-SAM pathway intermediates in iLet-7 and iLin28a mESCs after dox (n = 3). All error bars represent the s.e.m. from three independent measurements.

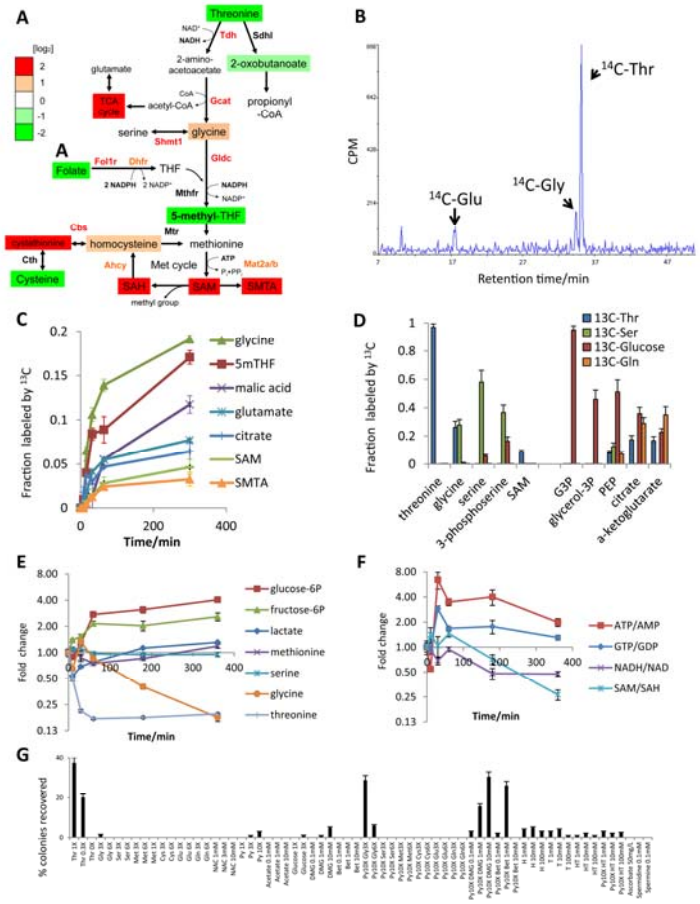

Fig. 2. Thr is catabolized to maintain the SAM/SAH ratio in mESCs. (**A**) Schematic of Thr-SAM pathway activity in pluripotent stem cells, relative to MEFs. (**B**) HPLC analysis of ^{14}C-labeled amino acids derived from [U-^{14}C]Thr in mESCs after 24h. Scintillation counts per minute (CPM) are plotted against retention time. (**C**) Fraction of intracellular metabolites derived from [U-^{13}C]Thr in mESCs over 5h, as measured by SRM analysis (n = 3). (**D**) Steady-state fraction of intracellular metabolites derived from [U-^{13}C]Thr, [U-^{13}C]Ser, [U-^{13}C]-glucose, or [U-^{13}C]Gln in mESCs after 48h, as measured by SRM analysis (n = 3). (**E**) SRM analysis of metabolite abundances in mESCs during 6h of Thr restriction, relative to time zero (n = 3). (**F**) SRM analysis of several metabolic ratios over a 6h time course, relative to time zero (n = 3). (**G**) Feeder-free mESCs were subjected to Thr restriction for 12h, then supplemented for 36h with the indicated metabolites at the given concentrations. Alkaline phosphatase-positive colonies were quantified and normalized to mESC colony numbers in normal mESC media (% colonies recovered). X denotes relative concentration with respect to DMEM medium. NAC, N-acetyl-cysteine. Py, pyruvate. DMG, dimethylglycine. Bet, betaine. H, hypoxanthine. T, thymidine. All error bars represent the s.e.m. from three independent measurements.

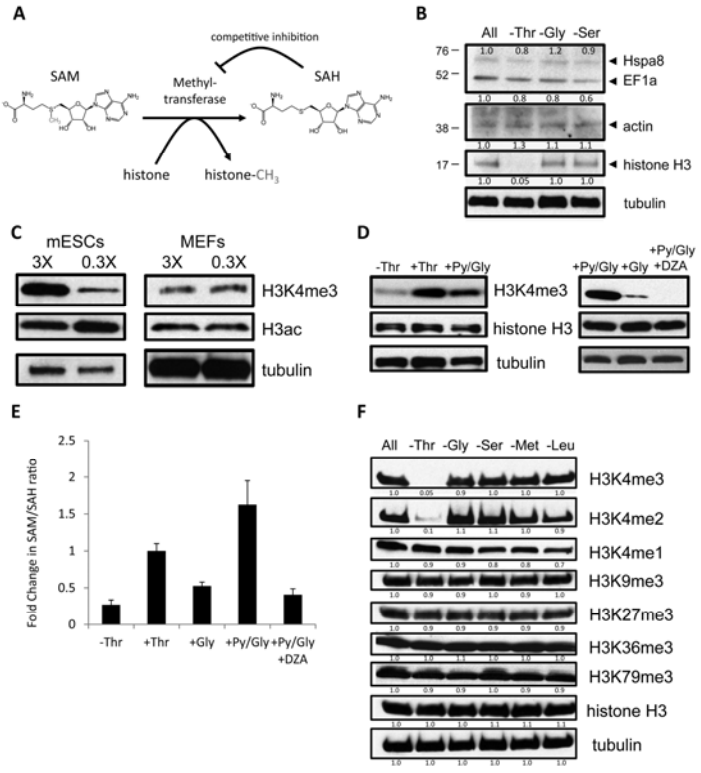

Fig. 3. Influence of Thr-SAM metabolism on H3K4 methylation. (**A**) Schematic of methyltransferase reactions. (**B**) Immunoblot analysis of proteins from mESCs with an antibody against methyl-lysine, after restriction indicated amino acids for 24h. (**C**) Immunoblot analysis of mESCs and MEFs for H3K4me3 and H3ac, when exposed to 3X and 0.3X concentrations for 48h. (**D**) Immunoblot analysis of mESCs for H3K4me3 after Thr restriction (0X) for 6h, then re-fed for 6h with indicated metabolites. DZA, 3-deaza-adenosine. (**E**) SAM/SAH ratio after Thr restriction (0X) for 6h, then re-fed for 6h with indicated metabolites. (**F**) Immunoblot analysis of mESCs for H3K4me3/2/1, K9me3, K27me3, K36me3, and K79me3, after restriction (0X) of indicated amino acids for 24h.

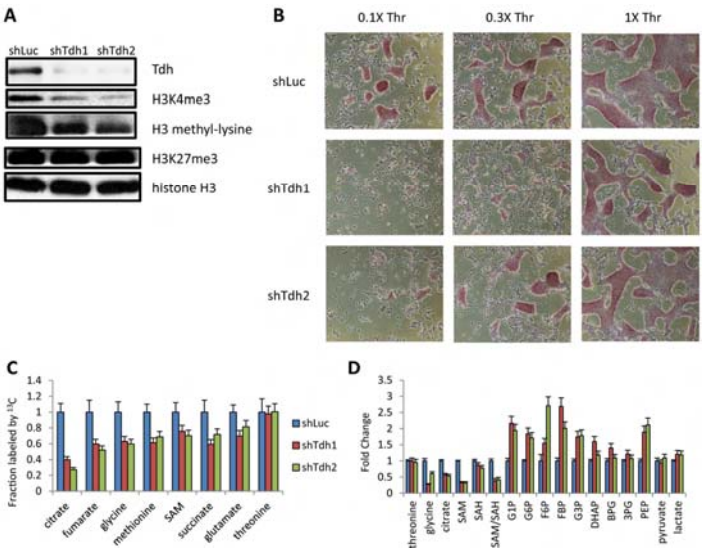

Fig. 4. Threonine dehydrogenase regulates the pluripotency of mESCs. (**A**) Immunoblot for Tdh, H3K4me3, H3K27me3, and pan-methyl-lysine in mESCs grown under 0.1X Thr, immediately after depletion of Tdh with 2 different shRNAs (shTdh), compared to a control shRNA targeting luciferase (shLuc). (**B**) Micrographs of alkaline-phosphatase-staining in mESCs after shTdh or shLuc, seeded at clonal density without feeder MEFs and after 48h of culture in 0.1X, 0.3X, and 1X Thr concentrations. (**C**) Steady-state fraction of intracellular metabolites derived from [U-^{13}C]Thr in mESCs after 24h, as measured by SRM analysis, after 48h dox-induction of shTdh or shLuc (n = 3). (**D**) SRM analysis of metabolite abundances in mESCs after 48h dox-induction of shTdh or shLuc (n = 3). All error bars represent the s.e.m. from three independent measurements.